

PAPER • OPEN ACCESS

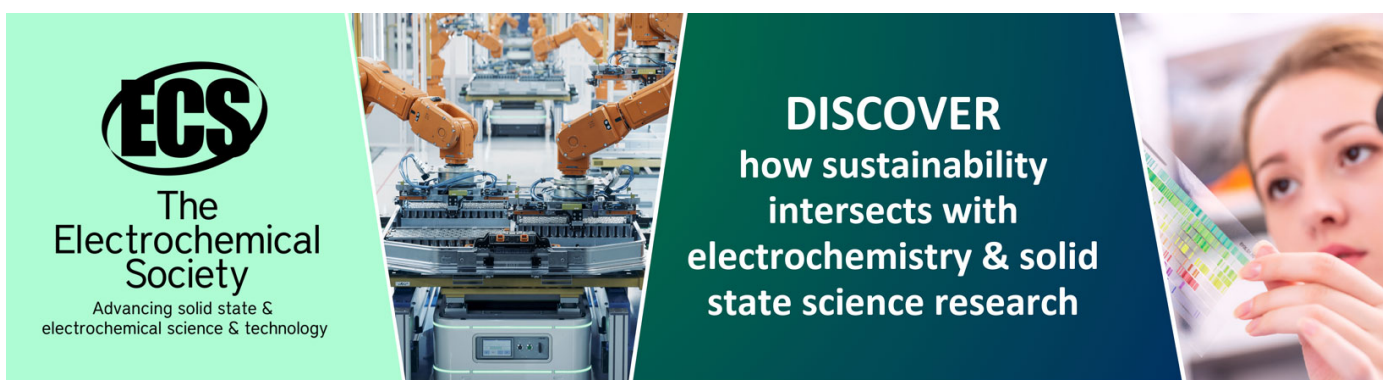
## Construction of simulation models for analyzing high-intensity shock effects in a spacecraft

To cite this article: S A Orlov *et al* 2020 *J. Phys.: Conf. Ser.* **1666** 012068

View the [article online](#) for updates and enhancements.

You may also like

- [Weight Optimization of Square Hollow Steel Trusses Using Genetic Algorithm](#)  
A.N. Ede, O.O. Oshokoya, J.O. Oluwafemi et al.
- [Strength and deformability of lightweight metal trusses with elements from cut I-beams](#)  
M Popova, M Sergeev, A Lukina et al.
- [Determination of the dynamic coefficient by the local damage of the element of steel trusses](#)  
Maria Berger and Alexandr Tusnin



**ECS**  
The  
Electrochemical  
Society  
Advancing solid state &  
electrochemical science & technology

**DISCOVER**  
how sustainability  
intersects with  
electrochemistry & solid  
state science research

# Construction of simulation models for analyzing high-intensity shock effects in a spacecraft

S A Orlov<sup>1</sup>, K A Matveev<sup>2</sup> and G I Rastorguev<sup>2</sup>

<sup>1</sup>ISS-Reshetnev company, 662972, Zheleznogorsk, Lenina str., 52, Russia

<sup>2</sup>Department of aircraft strength, Novosibirsk State Technical University, NSTU, 630073, Novosibirsk, K. Marx Avenue, 20, Russia :

E-mail: matveev@corp.nstu.ru

**Abstract.** In this paper, we consider the procedure for constructing stochastic models (based on processing of experimental data). These models allow to assess the propagation of high-intensity shock effects on the performance of unpressurized spacecrafts. The developed models are recommended for simulation of the load and the model of the system under study. Show the histograms of the distribution of total values of the impact reduction coefficient for typical structural joints, trusses, and shock isolators. The developed method allows to obtain an acceptable estimate of the propagation of high-intensity shock effects in the SC design.

## 1. Introduction

The sources causing impact of high intensity on the spacecraft (SC) are pyrotechnic devices of the launch vehicle (LV) and of the spacecraft: pyrolocks mounting SC to LV, solar panels locks, fixations of reflectors, etc [1-3]. It should be noted that modern SC are usually produced in the unpressurized performance. Various materials are used in the design of such SCs: metals (aluminum, steel, titanium), composite materials, cellular panels, etc. The device housings are mainly made of aluminum and magnesium alloys. As a result, it becomes quite difficult to develop a correct model of damping properties of structures, especially in high-intensity shock effects, when the range of interest to the developer is tens of kHz, and the damping in different frequency ranges may differ significantly. In this case, it is necessary to take into account the structural damping, damping properties of the materials as well as significant differences in the acoustic impedances of structural elements that are affected by the impact.

The results of the analysis of the spreading shock impacts on shell-and-rod structures (SC structures of unpressurized performance) are discussed in [4-6].

## 2. Processing of experimental results

In compliance with the results of the experimental work, the structural loading of unpressurised SCs was studied under the propagation of high-intensity shock effects. Both the spacecrafts' own pyrotechnic devices and special ones that create the necessary shock spectrum of accelerations were the sources of shock during such operations [7,8]. The impact was detected by single-axis accelerometers AR1017, AR1031 (mounted on a thread) in the zone where the impact source was located (0÷700mm) and three-axis accelerometers AR1020 at other control points. This made it possible to register accelerations in the



frequency range up to 20 kHz in the amplitude range up to 30000 g in the zone where the shock source is located, and in the frequency range up to 10 kHz in the amplitude range up to 10000g at other control points. While processing the measurement results, the instantaneous acceleration values and shock acceleration spectra were obtained. After that the maximum and minimum values were calculated for each loading case at different registration points. Moreover, the coefficients of the relationship between the impact point and the registration points were obtained as well as damping coefficients for the structure. Then, using regression analysis methods, a model was built that takes into account over of time and location on the analyzed structures.

As it is known, the shock loads of the explosive type are best described by the exponential function [9]. Therefore, for further analysis, we will use the equation describing the change in the impact (in the form of the impact acceleration spectrum) depending on the distance to the point source of impact [6]:

$$\text{SRS}(D_2) = \text{SRS}(D_1) \exp\left\{\left[-8 \cdot 10^{-4} f_n^{(2,4-0.105)}\right](D_2 - D_1)\right\}, \quad (1)$$

where  $\text{SRS}(D_1)$  is the amplitude of the shock spectrum of accelerations at the frequency  $f_n$  at a point at a distance  $D_1$  from the impact source;  $\text{SRS}(D_2)$  is the amplitude of the shock spectrum of accelerations at the frequency  $f_n$  at a point at a distance  $D_2$  from the impact source;  $D_1$  is the distance from the impact source;  $D_2$  is the distance to the point where the SRS is needed;  $f_n$  is the frequency at which the SRS is obtained.

The designs of various SC differ by rigidity, damping value, the method of attaching onboard equipment, etc. In addition, equation (1) gives an estimate with acceptable accuracy at the design stage ( $\pm 3\text{dB}$ ) only when the impact propagates over homogeneous structures (rods, plates, cylindrical shells, etc.). This equation adequately describes the propagation of impact on hermetic spacecrafts, for example, GLONASS – M.

The presence of special trusses in the SC for installing equipment, various types of joints in the power structure, and shock isolators also leads to a rapid change in the acoustic impedance of the system at these points and, accordingly, the shock spectrum of acceleration. It is obvious that the propagation of shock effects on the design of the SC can not be described by an equation that does not take into account such features.

Let us consider one of the possible modifications of equation (1). This equation includes components that lead to a rapid change in acceleration (the joint of structural elements, shock isolators, and special structures). Since the shock spectrum of accelerations is linear in relation to scalar multiplication, i.e. the shock spectrum of a signal multiplied by a scalar  $\alpha$  is equal to  $\alpha$  multiplied by the shock spectrum of this signal [10]. In other words, equation (1) can be written as follows:

$$\text{SRS}_i(D_{i2}) = \text{SRS}(D_{i1}) \left[ \prod^{k,l,m} (\alpha_i^{-k} \cdot \beta_i^{-l} \cdot \gamma_i^{-m}) \right] \exp\left\{\left[-\delta \cdot f_n^{(\mu \cdot f_n^{-\epsilon})}\right](D_{i2} - D_{i1})\right\}, \quad (2)$$

where  $\text{SRS}_i(D_{i2})$  is the amplitude of the shock spectrum of acceleration at frequency  $f_n$  at point  $i$  in the distance  $D_{i1}$  from the source of impact;  $D_{i1}$  is the distance from the source of impact to point  $i$ ;  $D_{i2}$  is the distance to point  $i$ , which is necessary to obtain  $\text{SRS}_i$ ,  $f_n$  is the frequency;  $\alpha_i$  is the coefficient reducing the impact of the joint design,  $k$  is the number of joints to point  $i$ ;  $\beta_i$  is the coefficient of reduction of impact

by truss  $i$ ,  $l$  is the number of farms to point  $i$ ;  $\gamma_i$  is the coefficient of reduction of impact shock isolator,  $m$  is the number of shock isolators to point  $i$ ;  $\delta$ ,  $\zeta$ ,  $\mu$  are coefficients that determine the attenuation of the impact when the impact propagates through the structure.

Figures 1-3 show the histograms of the distribution of total values of the impact reduction coefficient for typical structural joints, trusses, and shock isolators. As it can be seen from the figures, the coefficient  $\alpha_i$  varies in the range (1.5÷2.1),  $\beta_i$  is in the range (2.3÷3.2), and  $\gamma_i$  is in the range (5÷35).

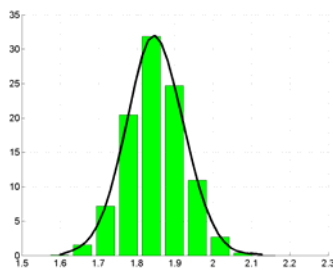


Figure 1. Distribution of impact reduction coefficient: construction joint

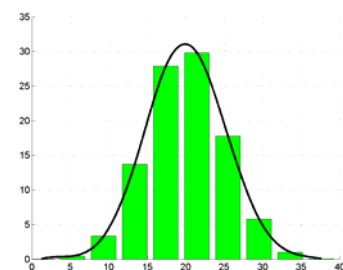
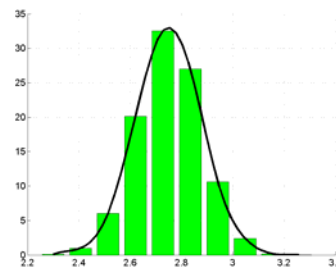


Figure 3. Distribution of impact reduction coefficient: shock isolator

The coefficients  $\delta$ ,  $\zeta$ , and  $\mu$  in formula (2) greatly depend on the design type and should be set in accordance with the results of processing the experimental data for the each class of SC. For example, for an unpressurized Glonass-K spacecraft, powered by cellular panels, they are as follows:  $\delta = 6.62 \cdot 10^{-4}$ ,  $\mu = 2.1$  and  $\zeta = 0.1$ . That is, the damping properties of the power structure of an unpressurized SC have significantly decreased relative to a hermetic SC of any close mass. It should be also noted that the coefficients  $\alpha_i$ ,  $\beta_i$ , and  $\gamma_i$  can be represented both as constants and as amplitude – frequency functions.

To estimate the change in the amplitude of shock acceleration over time, we will use the function proposed in [9] to describe the propagation of seismic waves:

$$a(t) = A_0 e^{-ct} \varphi(t) \eta(t), \quad (3)$$

where  $A_0$  and  $c$  are constants,  $\varphi(t)$  is a random function, and  $\eta(t)$  is a Heaviside function.

### 3. Evaluation of impact loads

For the analysis of the loading of the device as part of a SC under impact from a pyrotechnic (point) source, it is necessary to evaluate the changes in the impact on the device from time. This can be done using a formula similar to formula (3). As a result, we got an estimate of the loading of the SC structure at the place of installation of the device in the form of a shock acceleration spectrum that changes over time.

Let us consider the following formula (4):

$$S_i = \left[ S_{01} e^{-at_i} \sin(\omega t_i + \theta) + S_{02} e^{-bt_i} \sin(\nu t_i) + S_{03} e^{-ct_i} \sin(\zeta t_i) \right] \eta(t_i) + \psi(t_i), \quad (4)$$

where  $S_{01}$  is the maximum value of the acceleration amplitude at the trigger point of the pyrotechnic device in the frequency range 30÷500 Hz ;  $\omega$  is a narrow-band random frequency function, varying in the

range of 30÷500 Hz;  $\theta$  is a random constant in the range from 0 to  $\pi/2$ ;  $S_{02}$  is the maximum value of the acceleration amplitude at the trigger point of the pyrotechnic device in the frequency range of 0.5÷5 kHz;  $\nu$  is a high-frequency broadband random frequency function varying in the frequency range 0.5÷5 kHz;  $S_{03}$  is the maximum value of the acceleration amplitude at the trigger point of the pyrotechnic device in the frequency range of 5÷10 kHz;  $\zeta$  is a high-frequency broadband random frequency function varying in the frequency range of 5÷10 kHz;  $\eta(t_i)$  is the Heaviside function;  $\psi(t_i)$  is the normal stochastic noise;  $t_i$  is time in milliseconds.

Equation (4) was taken as a regression equation when processing the results of measurements on 21 SC. At each point of the structure for which experimental data are available, the acceleration dependence on time was calculated. Then, using formula (4) and regression analysis methods, a model was built for the change in acceleration from time to time at each control point. When analyzing accelerations, time dependencies were divided into three frequency sections: 30÷500 Hz, 0.5÷5 kHz, and 5÷10 kHz. The vibration effect was represented by the sum of a low-frequency vibration and two high-frequency components in the form of a combination of exponential and harmonic functions. The splitting was performed using a 5 - order Butterworth filter. The mathematical model of such a filter is closest to the real filters used in the measurements. Then the maximum and minimum values of the studied parameter were allocated for each term in formula (4). The stochastic noise level was assumed to be approximately equal to the noise level of the measuring equipment. This allowed us to obtain fairly simple dependences of the attenuation of the acceleration amplitude over time.

For the Glonass-K SC (when the solar cell locks are activated), the following coefficient values were obtained in formula (4):  $a = 0.5\div 0.6$ ;  $b = 0.8\div 0.9$ ;  $c = 0.9\div 1$ ;  $S_{01} = 600$  g;  $S_{02} = 5000$  g;  $S_{03} = 3000$  g;  $\psi(t_i)$  is the normal stochastic noise with the variance of 2.5% of the total process variance.

In equation (4), the transition from the shock amplitude  $S$  to the shock acceleration spectra SRS for equation (2) is not of considerable complexity and can be obtained by using any known algorithm, for example, [13].

Since the use of finite element modeling technology is ineffective at the stages of preliminary design (there are no real data on the design of the SC), we will use simulation technology to assess the loading of equipment located at various points in the structure [14]. Equation (2) is taken as the model of the system under study, and equation (4) is taken as the load. The load is set as a shock acceleration spectrum.

In general, the models of the load and the system under study consist of 14 random parameters that are taken into account when determining the SC loading. The calculation program was written in Excel.

When simulating the propagation of impact on the Glonass-K SC (operation on solar batteries) at the installation site of one of the devices at a distance of ~350mm from the lock, the maximum impact spectrum of accelerations in the range from 4200g to 6100g at frequencies from 3 kHz to 5 kHz was obtained. During the tests on this device, the shock level of 4700g was registered for the shock spectrum of accelerations. On the device installed on the truss, and located at a distance of ~750mm from the lock and after 2 joints, the calculated values did not exceed 200g, and the experimental 100g in the frequency range of 300÷500 Hz. The recommended safety margin for the shock acceleration spectrum is 2 (6 dB), for example, [15]. With this in mind, there is a good agreement between the calculated and experimental data.

So, the developed method allows to obtain an acceptable estimate of the propagation of high-intensity shocks in the SC.

## References

- [1] Calvi A. 2011 *Spacecraft Loads Analysis* (The Netherlands: ESA / ESTEC, Noordwijk)
- [2] Orlov S A, Matveev K A and Rastorguev G I 2017 *J. Phys.: Conf. Ser.* **894** 012131
- [3] Gladkiy V F 1975 *Strength, Vibration and Reliability of the Design of the Aircraft* (Moscow: Nauka) (in Russian)

- [4] Orlov A S and Shatrov A K 2005 *Vestn. SibSAU* **3** 153–5 (in Russian)
- [5] Van Ert D L 1985 *Survey of Pyroshock Prediction Methodology* (Institute of Environmental Sciences Pyrotechnic Shock Tutorial Program, 31st Annual Technical Meeting, Inst. Envir. Sc., Apr.-May)
- [6] *Pyroshock Test Criteria* 1999 NASA-STD-7003
- [7] Pat. 2394217 OF THE RUSSIAN FEDERATION, IPC G01M 7/08. Pyrotechnic device for creating shock effects /Orlov S A, Orlov A S, Publ. 10.07.2010, Bul. 19
- [8] Orlov S A 2011 *Nauch. Vestn. NSTU* **3** (44) 137–48
- [9] Bolotin V V 1979 *Random Fluctuations of Elastic Systems* (Moscow: Nauka) (in Russian)
- [10] ECSS-E-HB-32-25A. Space engineering. Mechanical shock design and verification handbook. 14 July 2015
- [11] Alimov O D and Manzhosov V K 1985 *Shock Effect. Propagation of Deformation Waves in Shock Systems* (Moscow: Nauka) (in Russian)
- [12] Orlov S A and Kopytov V I 2013 *Vestn. SibGAU* 1(47) 125–9 (in Russian)
- [13] Harris C M and Crede Ch E 1976 *Shock and Vibration Handbook* (New York: McGraw-Hill)
- [14] Gultaev A K 2001 *MatLab 5.3. Simulation in the Windows Interface* (St. Petersburg: KORONA print) (in Russian)
- [15] Product verification requirements for launch, upper-stage and space vehicles. MIL-STD-1540D, 15 January, 1999